

## Supporting Information

### High-rate, large capacity, and long life dendrite-free Zn metal anode enabled by trifunctional electrolyte additive with a wide temperature range

*Chuyuan Lin, Xuhui Yang, Peixun Xiong<sup>\*</sup>, Hui Lin, Lingjun He, Qi Yao, Mingdeng Wei, Qingrong Qian, Qinghua Chen<sup>\*</sup> and Lingxing Zeng<sup>\*</sup>*

C. Lin, X. Yang, H. Lin, L. He, Q. Yao, Prof. Dr. Q. Qian, Prof. Dr. Q. Chen, Prof. Dr. L. Zeng

Engineering Research Center of Polymer Green Recycling of Ministry of Education, College of Environmental Science and Engineering, Fujian Normal University, Fuzhou, Fujian 350007, People's Republic of China.

E-mail: zenglingxing@fjnu.edu.cn (L. Zeng); cqhuar@126.com (Q. Chen)

Dr. P. Xiong

School of Chemical Engineering, Sungkyunkwan University, Suwon-si, Gyeonggi-do 440-746, Republic of Korea.

E-mail: xiongpeixun@163.com (P. Xiong)

Prof. Dr. Q. Qian, Prof. Dr. Q. Chen, Prof. Dr. L. Zeng

Fujian Key Laboratory of Pollution Control & Resource Reuse, Fuzhou, Fujian 350007, People's Republic of China.

E-mail: zenglingxing@fjnu.edu.cn (L. Zeng); cqhuar@126.com (Q. Chen)

Prof. Dr. Q. Qian, Prof. Dr. Q. Chen, Prof. Dr. L. Zeng

Key Laboratory of Advanced Energy Materials Chemistry (Ministry of Education), College of Chemistry, Nankai University, Tianjin 300071, People's Republic of China.

Prof. Dr. M. Wei

Fujian Provincial Key Laboratory of Electrochemical Energy Storage Materials, Fuzhou University, Fuzhou, Fujian 350002, People's Republic of China.

**Keywords:** electrolyte additive, homogenize Zn deposition, stable interface pH, Zn anode

## 1. Experimental

### 1.1 Characterization

X-ray diffraction (XRD) performed on a Bruker D8 diffractometer by using filtered Cu-K $\alpha$  radiation under 40 kV and 20 mA. The microstructures of as-prepared samples were investigated by using scanning electron microscopy (SEM) (Hitachi 8010). X-ray photoelectron spectroscopy (XPS) spectra were carried out with an ESCALAB MARK II spherical analyzer with K $\alpha$  radiation as the X-ray source. Electron paramagnetic resonance measurement was collected on MS 5000. Raman spectra were conducted on DXR2xi with a laser at wavelength of 532 nm.

### 1.2 Electrochemical Measurements

Tafel plots were scanned within  $-0.8$  and  $-1.1$  V at  $1 \text{ mV s}^{-1}$  with the reference electrode (Ag/AgCl electrode), and the Zn plates as the counter electrode and the working electrode in three-electrode setups. The chronoamperometry (CA) transient curves were recorded at  $-150$  mV fixed overpotential. Linear sweep voltammetry (LSV) tests were accomplished with a scanning velocity of  $10 \text{ mV s}^{-1}$ . The above test was implemented in  $\text{ZnSO}_4$  and  $\text{ZnSO}_4$ :  $\text{CH}_3\text{COONH}_4$  electrolytes. Electrochemical impedance spectroscopy (EIS) studies were measured at a sinusoidal perturbation of 5 mV and in the frequency range of 1 mHz~100 kHz.

### 1.3 Computational Methods

Total energy calculations were conducted through density functional theory (DFT) using the Vienna *ab initio* Simulation Package (VASP) using the projector-augmented wave (PAW) method.<sup>[S1]</sup> The Perdew-Burke-Ernzerhof (PBE)

approximation based on the generalized gradient approximation (GGA) was used to determine the influence of the exchange-correction potentials.<sup>[S2, S3]</sup> A plane-wave cutoff energy was set as 800 eV. A Monkhorst-Pack K-point sampling of 18×18×6 was used for the crystalline Zn unit cell. To save the computational resources, the Zn (0001) surface was modelled by a five-layer 5×5 surface supercell (25 Zn atoms per layer) considering only considering the  $\Gamma$  point, and the convergence criteria for the ionic relaxation and the electronic self-consistent electronic calculation were set to 0.03 eV/Å and 10<sup>-5</sup> eV, respectively. In addition, a vacuum of 25 Å was used to avoid the interaction between periodically neighbour slabs. A dispersion-corrected DFT method (DFT-D2) was adopted for the long-range dispersion correction.<sup>[S4]</sup> For absorption systems, the two top atomic layers were relaxed and the other three bottom layers were fixed.

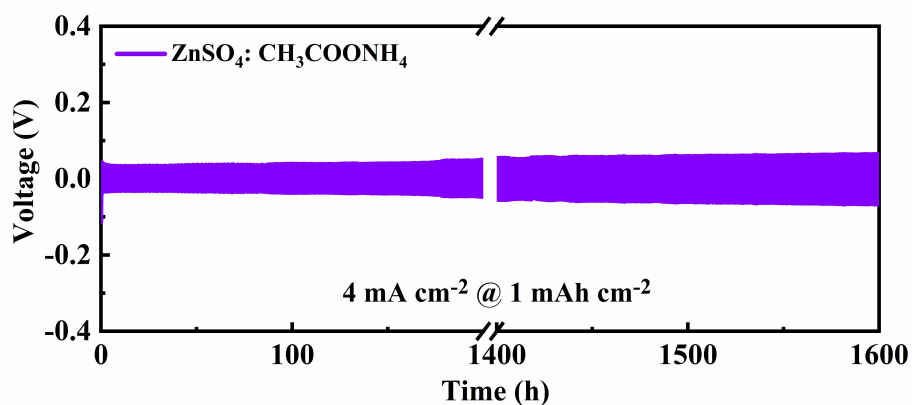


**Fig. S1** Cycling performance of Zn||Zn symmetrical cells with ZnSO<sub>4</sub>: CH<sub>3</sub>COONH<sub>4</sub> electrolyte at 4 mA cm<sup>-2</sup> for 1 mAh cm<sup>-2</sup>.

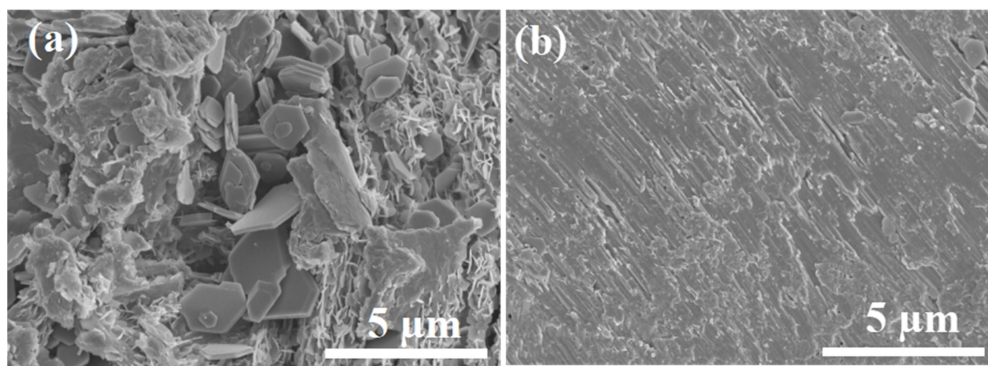


**Fig. S2** Scanning electron microscopy (SEM) images of Zn||Zn symmetrical cells cycled 200 h: (a) ZnSO<sub>4</sub> electrolyte; (b) ZnSO<sub>4</sub>: CH<sub>3</sub>COONH<sub>4</sub> electrolyte.

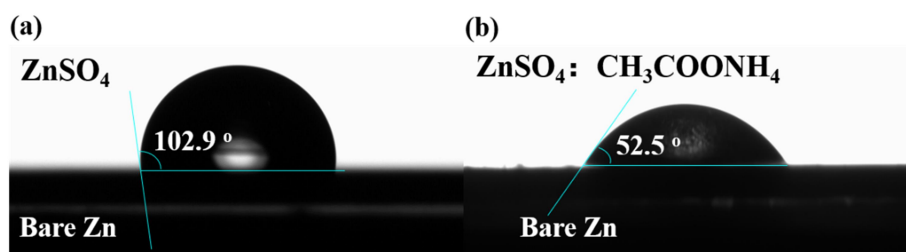


**Fig. S3** The contact angle of Zn anode after cycling in (a) ZnSO<sub>4</sub> electrolyte and (b) ZnSO<sub>4</sub>: CH<sub>3</sub>COONH<sub>4</sub> electrolyte.

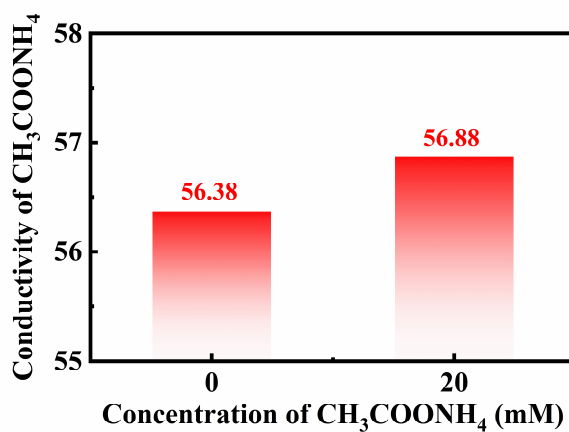


**Fig. S4** The conductivity of electrolyte with / without CH<sub>3</sub>COONH<sub>4</sub>.



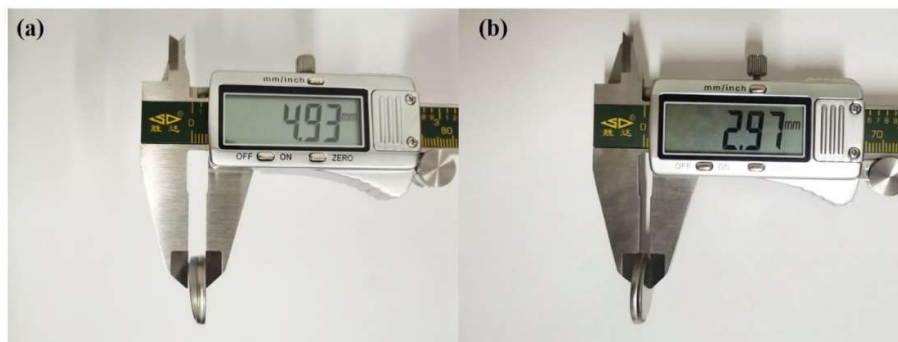


**Fig. S5** The photos of the cycled Zn||Zn button cells (a) without or (b) with  $\text{CH}_3\text{COONH}_4$  after 50 cycles at  $20 \text{ mA cm}^{-2}$  for  $5 \text{ mAh cm}^{-2}$ .

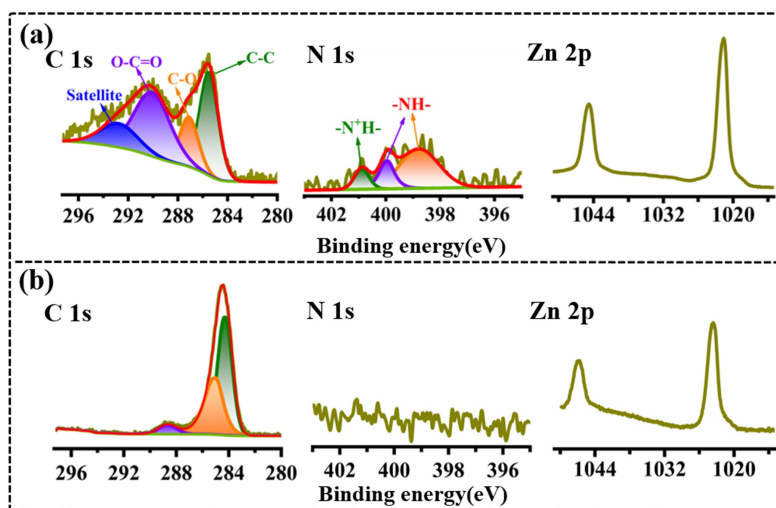


**Fig. S6** XPS spectra of C 1s, N 1s and Zn 2p of Zn-electrode after 5 cycles at  $1 \text{ mA cm}^{-2}$ : (a)  $\text{ZnSO}_4$ :  $\text{CH}_3\text{COONH}_4$  electrolyte; (b)  $\text{ZnSO}_4$  electrolyte.

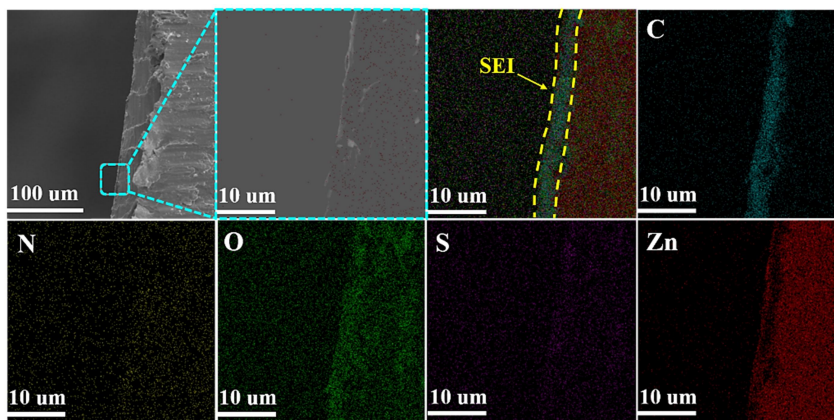


**Fig. S7** the scanning electron microscope - energy dispersive spectroscopy (SEM-EDS) images of the cross section of Zn anode after 10 cycles at  $1 \text{ mA cm}^{-2}$ .

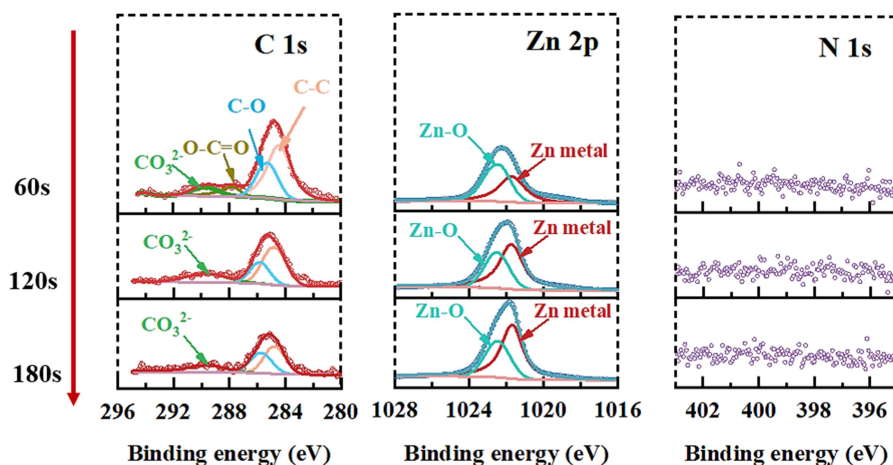


**Fig. S8** XPS of C 1s, Zn 2p, and N 1s, which are displayed in rows, with corresponding durations of Ar<sup>+</sup> sputtering in columns.

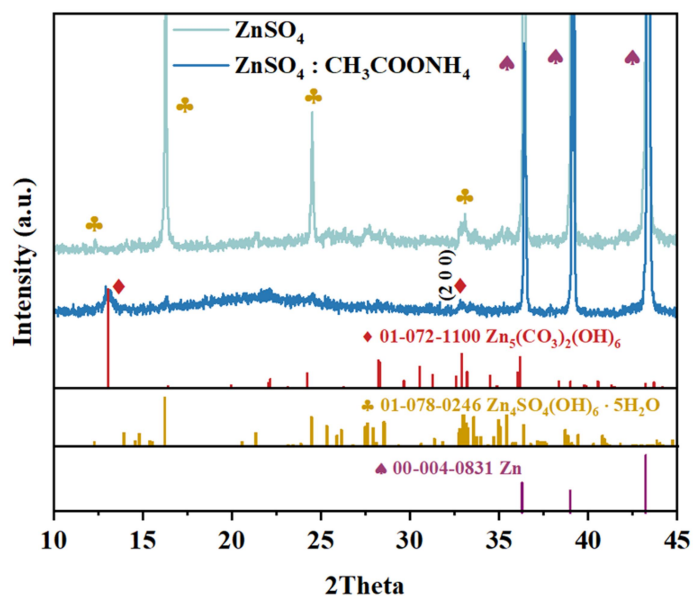


**Fig. S9** XRD patterns of Zn anode after 3 cycles in ZnSO<sub>4</sub> and ZnSO<sub>4</sub>: CH<sub>3</sub>COONH<sub>4</sub> electrolytes.

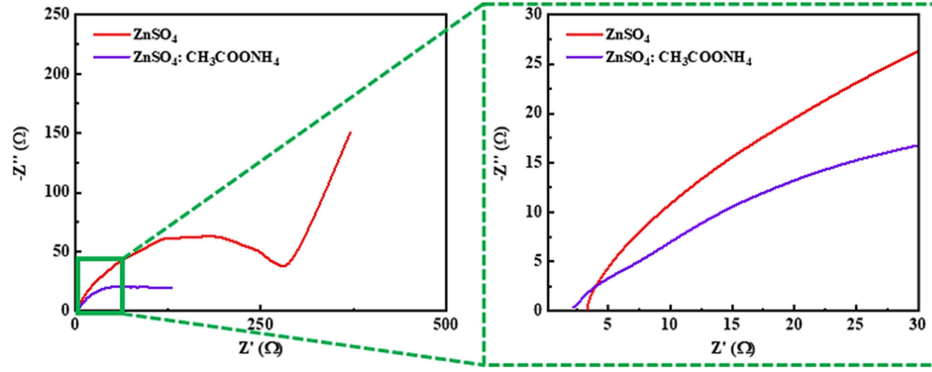


**Fig. S10** EIS spectra of the Zn||Zn cells after 5 cycles at  $1 \text{ mA cm}^{-2}$  for  $1 \text{ mAh cm}^{-2}$ .

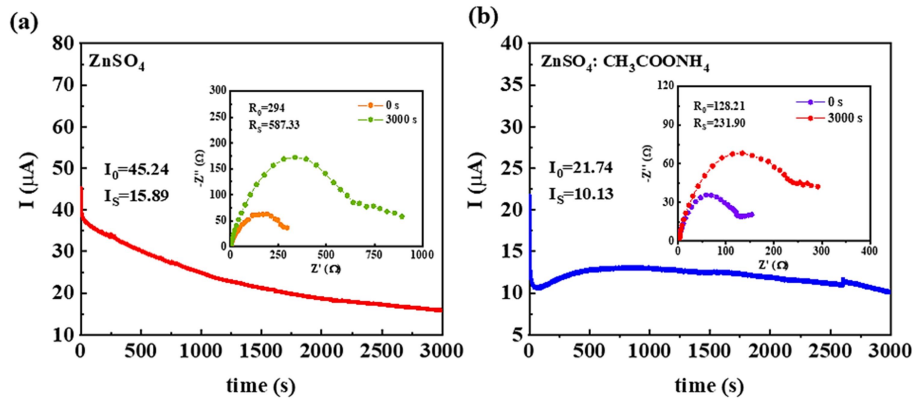


**Fig. S11** Measurements of  $\text{Zn}^{2+}$  transference number. Current-time plots of Zn symmetric cells with (a) bare Zn and (b) SEI-Zn after polarization at 15 mV for 3000 s. The insets are the impedance spectra before and after polarization. The transference number of  $\text{Zn}^{2+}$  ( $t_{\text{Zn}^{2+}}$ ) was evaluated by the following equation<sup>[S5]</sup>:

$$t_{\text{Zn}^{2+}} = \frac{I_s(\Delta V - I_0 R_0)}{I_0(\Delta V - I_s R_s)}$$

where  $\Delta V$  is the constant polarization voltage applied (15 mV here),  $I_0$  and  $R_0$  are the initial current and resistance, and  $I_s$  and  $R_s$  are the steady-state current and resistance, respectively.

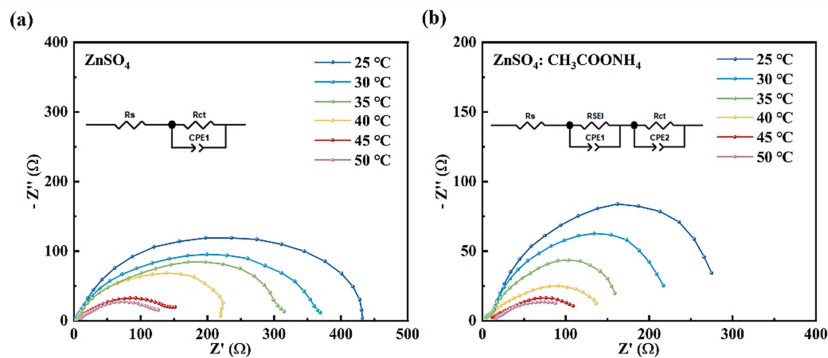


**Fig. S12** The corresponding Nyquist plots of Zn symmetric cells in (a)  $\text{ZnSO}_4$  electrolyte and (b)  $\text{ZnSO}_4\text{: CH}_3\text{COONH}_4$  electrolyte at different temperatures.

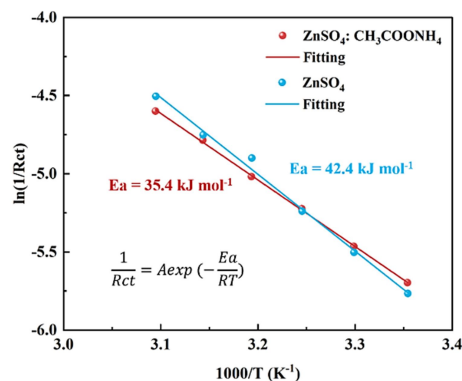


**Fig. S13** Arrhenius curves of Zn symmetric cells at different temperatures (inset shows the related equation to calculate the activation energy ( $E_a$ )).

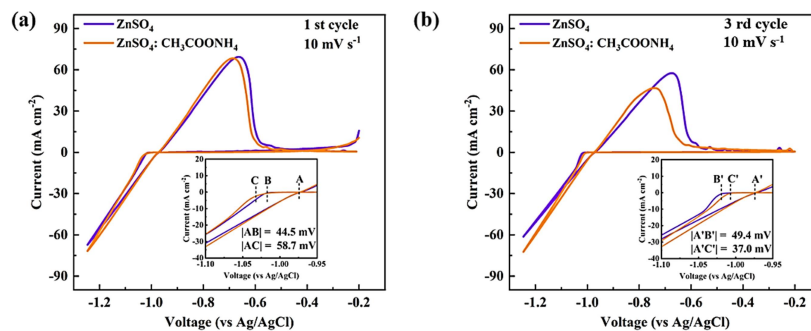


**Fig. S14** The cyclic voltammetry (CV) curves of Zn plating/stripping on Ti foil with different electrolytes ( $10 \text{ mV s}^{-1}$ ).

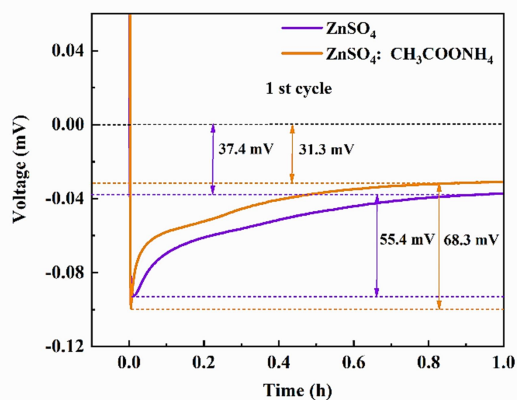


**Fig. S15** Nucleation overpotential (NOP) based on the Ti substrate with or without  $\text{CH}_3\text{COONH}_4$  at a current density of  $2 \text{ mA cm}^{-2}$ .

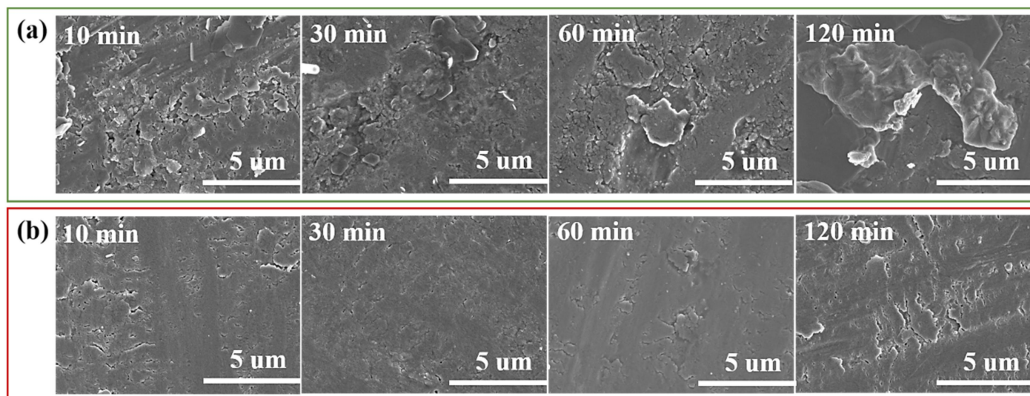


**Fig. S16** The SEM image of Ti foil after cycling for 10, 30, 60 and 120 min in (a)  $\text{ZnSO}_4$  electrolyte and (b)  $\text{ZnSO}_4 : \text{CH}_3\text{COONH}_4$  electrolyte at  $2 \text{ mA cm}^{-2}$ .

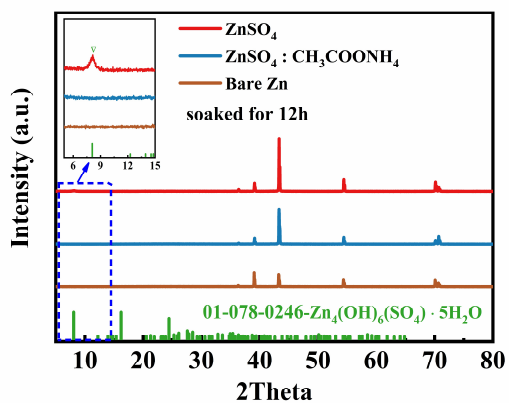


**Fig. S17** XRD patterns of pristine Zn foil and Zn-electrode soaked for 12 h in different electrolytes.

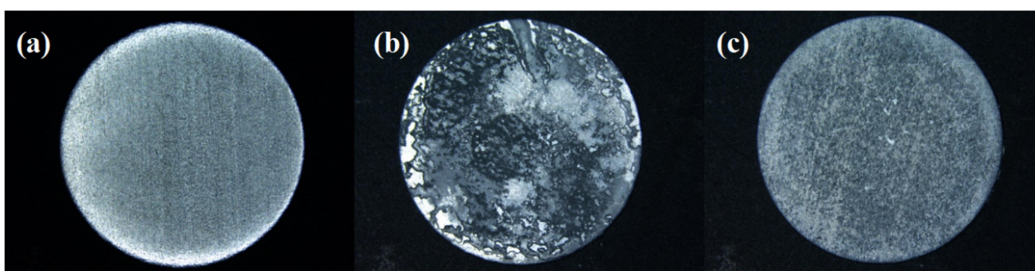


**Fig. S18** Photos of (a) pristine Zn foil, (b) Zn-electrode in  $\text{ZnSO}_4$ , and (c) Zn-electrode in  $\text{ZnSO}_4$ :  $\text{CH}_3\text{COONH}_4$  after 20 cycles at  $5 \text{ mA cm}^{-2}$  for  $5 \text{ mAh cm}^{-2}$ .

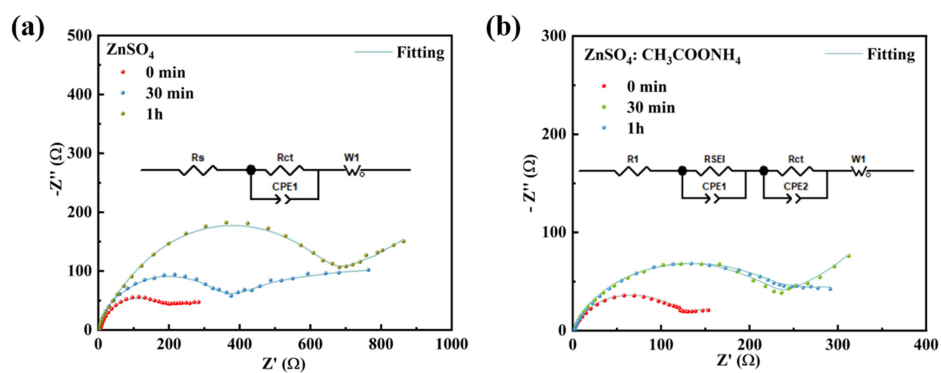


**Fig. S19** The EIS fitted curves of the symmetric batteries in difference electrolyte.

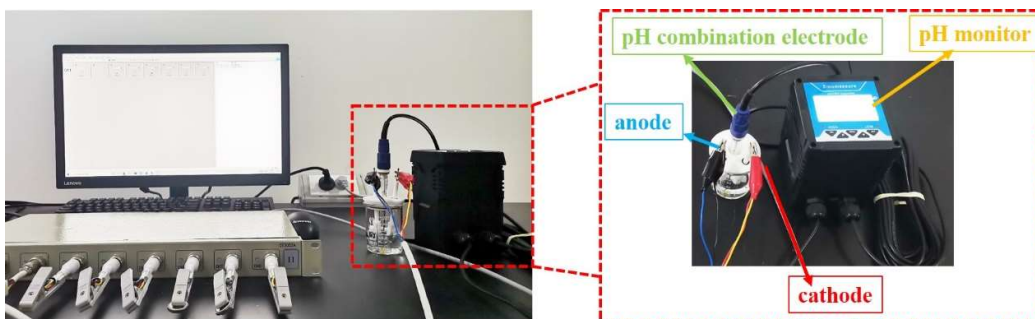


**Fig. S20** Digital image of the assembled equipment for studying pH change of electrolytes during cycling.



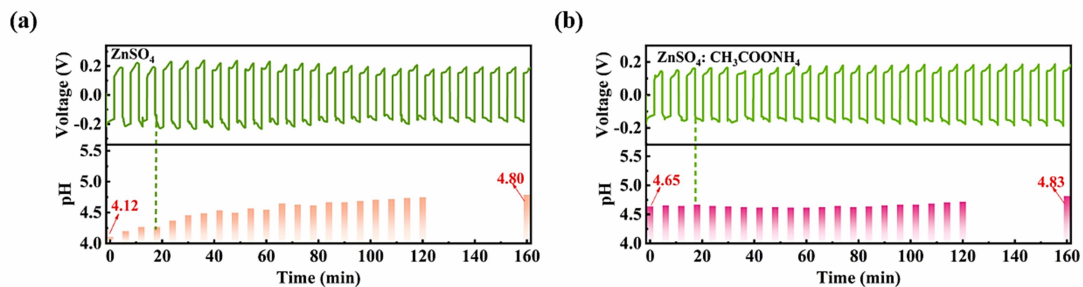


**Fig. S21** The pH monitoring of (a)  $\text{ZnSO}_4$  electrolyte and (b)  $\text{ZnSO}_4:\text{CH}_3\text{COONH}_4$  electrolyte of symmetric batteries cycling at  $20 \text{ mA cm}^{-2}$ , respectively.

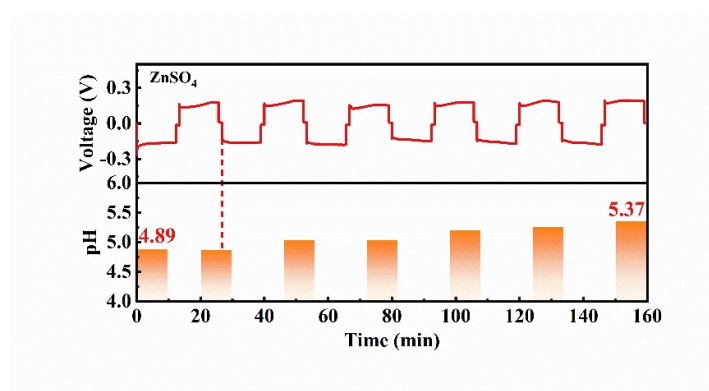


**Fig. S22** The pH monitoring of  $\text{ZnSO}_4$  electrolyte of symmetric batteries cycling at  $5 \text{ mA cm}^{-2}$  in ice water bath.

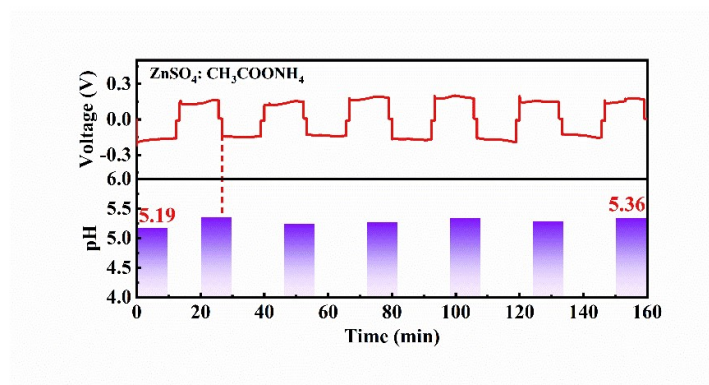


**Fig. S23** pH monitoring of  $\text{ZnSO}_4:\text{CH}_3\text{COONH}_4$  electrolyte of symmetric batteries cycling at  $5 \text{ mA cm}^{-2}$  in ice water bath.

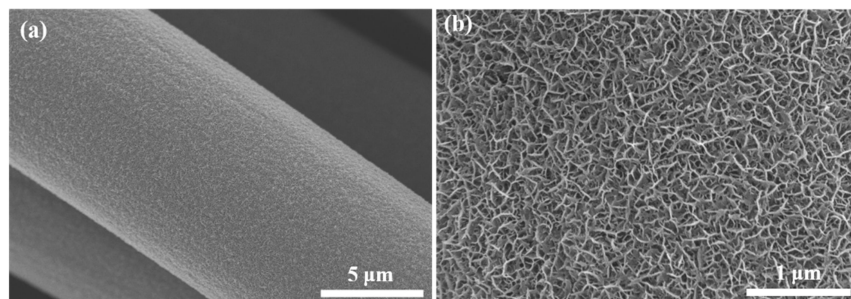


**Fig. S24** SEM images of MnO<sub>2</sub> cathode.

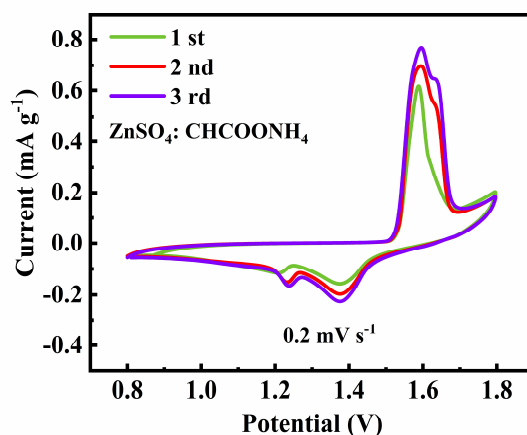


**Fig. S25** CV curves of Zn || MnO<sub>2</sub> full cells in ZnSO<sub>4</sub>: CH<sub>3</sub>COONH<sub>4</sub> electrolyte at 0.2 mV s<sup>-1</sup>.

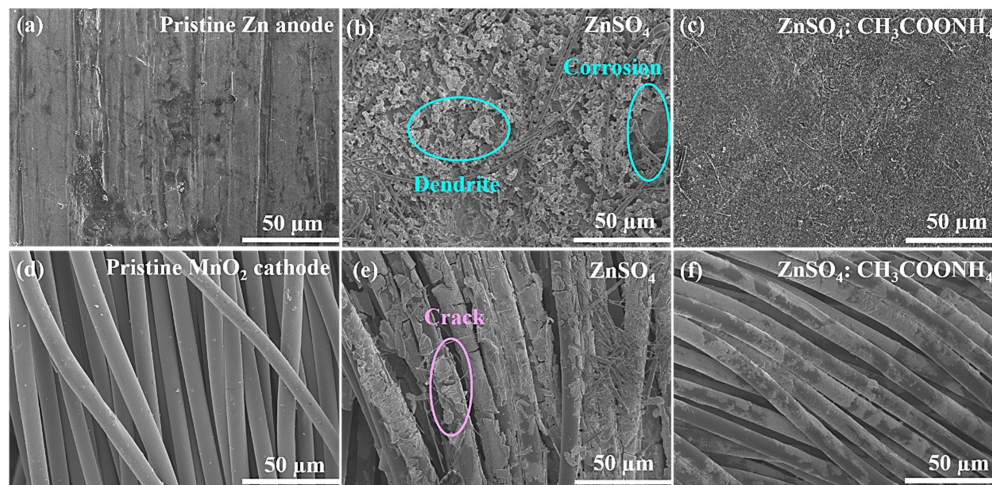


**Fig. S26** SEM images of the Zn || MnO<sub>2</sub> full cells after 100 cycles in different electrolyte: (a) Zn anode and (d) MnO<sub>2</sub> cathode before cycling; (b) Zn anode and (e) MnO<sub>2</sub> cathode after cycling in ZnSO<sub>4</sub> electrolyte; (c) MnO<sub>2</sub> cathode and (f) Zn anode after cycling in ZnSO<sub>4</sub>: CH<sub>3</sub>COONH<sub>4</sub> electrolyte.



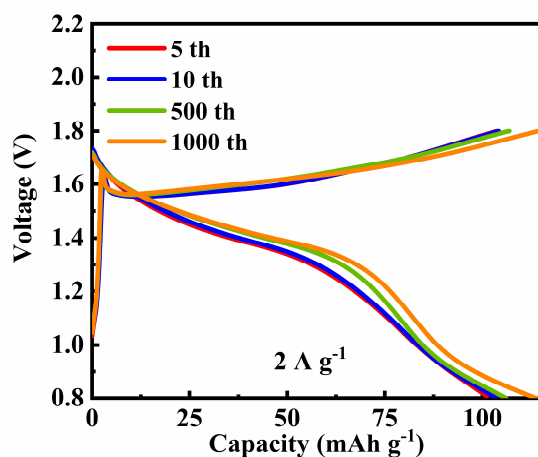


**Fig. S27** Charge and discharge curves of Zn || MnO<sub>2</sub> full cells at 2 A g<sup>-1</sup> for different cycles.

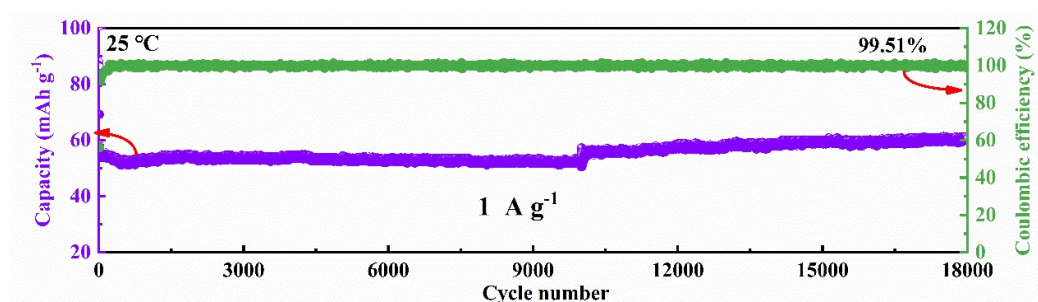


**Fig. S28** The coulombic efficiency and long-term cycling performance of Zn||Ac capacitors in ZnSO<sub>4</sub>: CH<sub>3</sub>COONH<sub>4</sub> electrolyte at 25 °C.

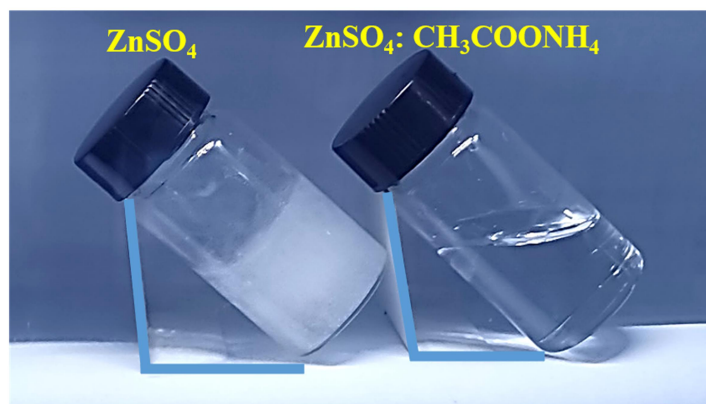


**Fig. S29** The digital photos for physical state of ZnSO<sub>4</sub> electrolyte and ZnSO<sub>4</sub>: CH<sub>3</sub>COONH<sub>4</sub> electrolytes in -10 °C.

**Video S1** Operando compressed fast forward optical video of Zn anodes observed in 2 M  $\text{ZnSO}_4$  and  $\text{ZnSO}_4$ :  $\text{CH}_3\text{COONH}_4$  electrolytes for 30 mins.

## References

- [S1] J. Hafner, *J. Comput. Chem.* **2008**, 29, 2044.
- [S2] G. Kresse, J. Hafner, *Phys. Rev. B* **1993**, 48, 13115.
- [S3] J. P. Perdew, K. Burke, Y. J. P. r. B. Wang, *Phys. Rev. B* **1996**, 54, 16533.
- [S4] S. Grimme, *J. Comput. Chem.* **2006**, 27, 1787.
- [S5] X. Zeng, J. Mao, J. Hao, J. Liu, S. Liu, Z. Wang, Y. Wang, S. Zhang, T. Zheng, J. Liu, P. Rao, Z. Guo, *Adv. Mater.* **2021**, 33, 2007416.